Liquid-Phase Thermodynamic Properties for Propane (1), *n*-Butane (2), and Isobutane (3)

Yohei Kayukawa,*,† Masaya Hasumoto,†,‡ Yuya Kano,† and Koichi Watanabe†

School of Science for Open and Environmental Systems, Graduate School of Science and Technology, Keio University, 3-14-1, Hiyoshi, Kohoku-ku, Yokohama 223-8522, Japan

Hydrocarbons (HCs) are environmentally friendly natural refrigerants and are expected to be promising alternative candidates to replace some currently used halogenated hydrocarbon refrigerants. Some available data sets for HCs used to formulate the equations of state (EoS) for them are relatively old, so we point out that new data with less uncertainty are expected to play an essential role in updating the EoS for HCs. Therefore, a set of *PVT* property measurements for hydrocarbon refrigerants including propane, *n*-butane, and isobutane was conducted in the present study. A newly developed vibrating-tube densimeter was employed for the measurements, and then a total of 430 liquid *PVT* properties were obtained, including those at the saturation boundaries. The measurement range is (240 to 380) K for temperature and up to 7 MPa for pressure. The measurement uncertainty is about 3 mK for temperature, 0.26 kPa + 0.022% for pressure, and 0.1 kg·m^{-3} + 0.024% for density. The present data were compared with available thermodynamic models that are currently considered to be the most reliable. A set of modified Tait equations of state for the liquid phase are also discussed.

Introduction

Hydrocarbons (HCs) are expected to be promising alternative candidates to replace some fluorinated hydrocarbon refrigerants such as CFCs (chlorofluorocarbons), HCFCs (hydrochlorofluorocarbons), and HFCs (hydrofluorocarbons). Because their global warming potential (GWP) is negligible, they are regarded as environmentally friendly and good cost-performance refrigerants, despite their flammability. Some household refrigerators from manufacturers in Europe and even Japan have already been developed .

However, it is needless to say that the thermodynamic models for HCs play an essential role in cycle-performance prediction, various kinds of design for equipment, and the selection of refrigerants. Recently, Miyamoto and Watanabe developed a set of multiproperty equations of state (EoS) for propane,[1] *n*-butane,[2] and isobutane.[3] These EoS were employed by the latest version of the thermodynamic-property calculation software REFPROP (version 7.0)[4] to supersede those developed earlier by Younglove and Ely.[5] Concerning the input data used for these models, however, some of them are relatively old.

Hence, we point out that an additional set of *PVT* data for these hydrocarbons are important to confirm the reproducibility and soundness of the available thermodynamic models. In the present study, we have intended to measure *PVT* properties for propane, *n*-butane, and isobutane with a newly developed density-measurement system with the aid of a vibrating-tube densimeter. More than 400 data points including liquid-phase *PVT* properties, vapor pressures, and saturated-liquid densities were obtained in this study. These were compared with the above-mentioned EoS by Miyamoto and Watanabe[1−3] to examine the representation of the EoS. On the basis of the present measurements, the modified Tait EoS was also developed to interpolate the present data.

* To whom correspondence should be addressed. Present affiliation: Fluid Properties Section, Material Properties and Metrological Statistics Division, National Metrology Institute of Japan, National Institute of Advanced Industrial Science and Technology, AIST Tsukuba Central 3, Tsukuba 305-8563, Japan. E-mail: kayukawa-y@aist.go.jp. Tel: +8145-563-1141. Fax: +81-45-566-1720.
† Keio University.
‡ Present affiliation: Builiding Systems Solution Department, Builiding Systems Development Center, Matsushita Electric Works, Ltd., 1048 Kadoma, Osaka 571-8686, Japan.

Experimental Section

Setup. The density-measurement system used in the present study was developed by us.[6] A detailed description of the apparatus has been given.[6,7]

Figure 1 illustrates a schematic diagram of the present measurement system. The main part of the system is a pressure−density measurement unit, and its outlook is shown in Figure 2. A vibrating-tube densimeter (VD) is suspended by four springs from the L-shaped frame. A digital pressure gauge (PT, 31 K, Paroscientific, Co.) is also supported by the frame and directly connected to the uppper port of the densimeter. There were four valves (V1−V4) within the pressure−density-measurement system. The variable-volume vessel (VB) is placed between valves V1 and V2 and connected to the lower port of the densimeter. The sample fluid was discharged from the upper port of the densimeter through the expansion space between valves V3 and V4.

We have employed a commercially available densimeter (DMA512, Anton Paar, K. G.). Its densimeter cell was removed, however, from the densimeter box and attached to a balance weight (5.5 kg) made of stainless steel.

The sample pressure and density are regulated by changing the inner volume of the unit by means of the variable-volume vessel and measured by the densimeter and the pressure gauge.

Measurements were made by immersing the pressure−density measurement system into the bath fluid (silicone oil) of the thermostatic bath (LB). It should be noted that only the pressure gauge (PT) is located above the meniscus of the bath fluid in order to protect the pressure gauge from

10.1021/je049672l CCC: $30.25 © 2005 American Chemical Society
Published on Web 02/05/2005

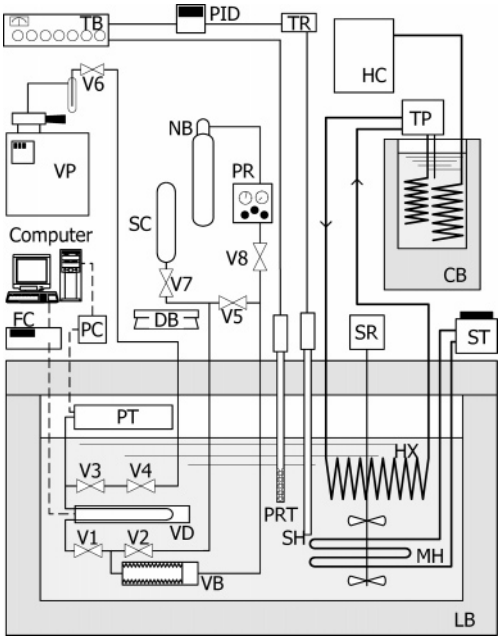

Figure 1. Schematic diagram of the experimental apparatus: VD, vibrating-tube densimeter cell; FC, frequency counter; PT, digital pressure gauge; PC, pressure computer; VB, variable-volume vessel with metallic bellows; PR, pressure regulator; NB, nitrogen gas bomb; SC, sample-supplying cylinder; DB, digital balance; VP, vacuum pump; PRT, standard platinum resistance thermometer; TB, thermometer bridge; LB, liquid bath; PID, PID controller; TR, thyristor regulator; SH, subheater; MH, main heater; ST, slide transformer; SR, stirrer; HX, heat exchanger; TP, temperature regulator pump; CB, cooling bath; HC, handy cooler; V1−7, valves.

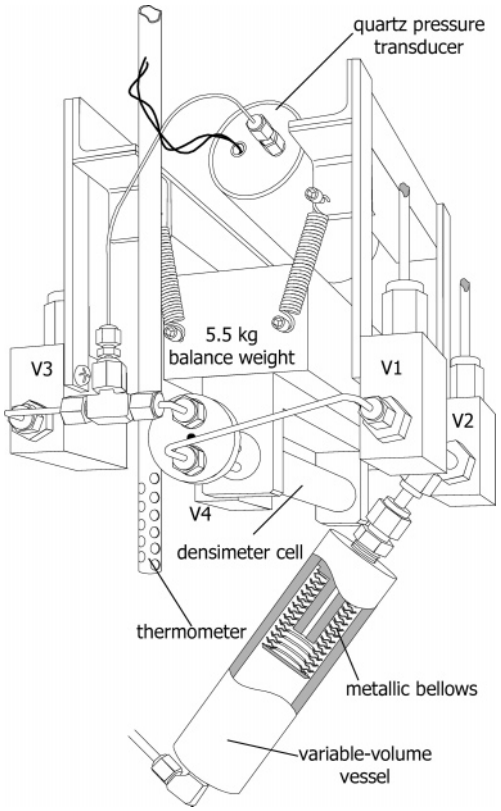

Figure 2. Drawing of the pressure−density measurement unit.

the bath fluid. The sample temperature was regarded as being equivalent to the bath-fluid temperature, and it was feedback controlled by means of a PID-controlled subheater (SH) associated with a PID controller (PID), a thermometer bridge (TB), and a standard platinum resistance thermometer (PRT) inserted in the vicinity of the densimeter.

Calibration and Uncertainty. It should be noted that, in the present study, measurement uncertainties were evaluated along the ISO guideline[8] where the coverage factor was $k = 2$.

The standard platinum resistance thermometer used in the present measurement was calibrated against ITS-90. The bath-fluid temperature was kept within a fluctuation of ±1 mK so that the temperature-measurement uncertainty becomes 3 mK for temperatures less than 360 K. At temperatures above 360 K, the uncertainty approaches 7 mK.

The digital pressure gauge was calibrated against a dead-weight piston gauge. The difference in the displayed pressure was corrected as a function of temperature and pressure. Because that difference does not change very much with absolute pressure but primarily depends on temperature, the approximate error in the digital pressure gauge is known by measuring under vacuum. The repeatability of the digital pressure gauge is about ±0.01%, whereas the pressure-measurement uncertainty of the dead-weight piston gauge is ±0.005%. By summing these uncertainties, the present pressure-measurement uncertainty was evaluated to be

$$U = 0.26\ \text{kPa} + 0.00022P \tag{1}$$

where the coverage factor is $k = 2$.

In the present study, the density was evaluated from the vibrational period of the U tube of the densimeter on the basis of the calibration function developed. This function was determined by measuring the vibrational period of water. The non- linearity of the relation between τ^2 and ρ is corrected by introducing a nonlinear calibration model. Along the present calibration function, density, ρ, is evaluated as

$$\rho = A\frac{(1+\mu)x}{1-\mu x} \tag{2}$$

$$x = \left(\frac{\tau^2}{\tau_0^{\,2}}\right) - 1 \tag{3}$$

$$A = (a_1 + a_2 T^{*0.75} + a_3 T^{*3})(1 - a_4 P^*) \tag{4}$$

$$P^* = \frac{P/\text{kPa}}{7000} \tag{5}$$

$$T^* = \frac{T/\text{K}}{400} \tag{6}$$

where the periodical parameter, x, was obtained from the vibrational period, τ, and that under vacuum, τ_0, was defined in eq 3. Parameter τ_0 was obtained in the same experiment for the sample by evacuating the sample from the measurement system. However, A is a proportional parameter and was determined by calibration with a fluid (water) of known density. We have correlated this parameter as a function of temperature and pressure given in eq 4. Parameter μ is a device-dependent constant that denotes the nonlinearity of the relation between τ^2 and ρ and was determined to be $\mu = 0.0030 \pm 0.0005$ by comparing the density of water and isooctane at the same temperature and pressure. The density measurement uncertainty was evaluated as

$$U = 0.1\ \text{kg·m}^{-3} + 0.00024\rho \tag{7}$$

Table 1. Experimental *PVT* Data for Propane

T/K	P/kPa	ρ/kg·m^{-3}	T/K	P/kPa	ρ/kg·m^{-3}	T/K	P/kPa	ρ/kg·m^{-3}
240.000	147.9	570.28[a]	240.000	7043.3	578.91	240.000	6523.2	578.30
240.000	6018.3	577.69	240.000	5475.7	577.04	240.000	4957.8	576.41
240.000	4504.5	575.85	240.000	4045.7	575.29	240.000	3513.0	574.62
240.000	2999.9	573.98	240.000	2477.9	573.32	240.000	1978.3	572.68
240.000	1522.4	572.08	240.000	1044.8	571.46	240.000	527.3	570.78
240.000	147.9	570.28[a]	250.000	7010.3	567.78	250.000	6543.5	567.17
250.000	5999.9	566.46	250.000	5495.4	565.78	250.000	5045.1	565.17
250.000	4478.5	564.40	250.000	3993.1	563.74	250.000	3503.7	563.05
250.000	3016.9	562.38	250.000	2524.1	561.67	250.000	2008.3	560.93
250.000	1508.3	560.20	250.000	1008.1	559.47	250.000	513.8	558.73
250.000	217.7	558.29[a]	260.000	310.3	545.77[a]	260.000	7048.9	556.40
260.000	6522.8	555.62	260.000	6028.2	554.89	260.000	5513.9	554.12
260.000	5014.5	553.38	260.000	4498.9	552.58	260.000	4020.0	551.84
260.000	3513.3	551.04	260.000	3012.1	550.24	260.000	2504.5	549.42
260.000	1999.7	548.60	260.000	1503.5	547.77	260.000	1013.8	546.96
260.000	506.6	546.10	270.000	429.6	532.67[a]	270.000	7024.1	544.55
270.000	6525.8	543.74	270.000	6021.1	542.91	270.000	5504.7	542.05
270.000	5023.8	541.26	270.000	4488.2	540.32	270.000	4018.8	539.50
270.000	3497.1	538.57	270.000	3017.5	537.70	270.000	2499.6	536.75
270.000	2005.4	535.83	270.000	1510.4	534.87	270.000	1012.9	533.91
270.000	504.7	532.93	280.000	7034.7	532.51	280.000	6522.6	531.56
280.000	5982.8	530.51	280.000	5443.4	529.45	280.000	4963.1	528.50
280.000	4527.5	527.65	280.000	4049.7	526.68	280.000	3519.3	525.60
280.000	3032.9	524.61	280.000	2513.0	523.49	280.000	1964.2	522.28
280.000	1466.1	521.15	280.000	1000.0	520.10	290.000	768.6	504.75[a]
290.000	7049.2	519.81	290.000	6525.4	518.70	290.000	5957.4	517.46
290.000	5531.4	516.52	290.000	5036.3	515.41	290.000	4476.9	514.12
290.000	4018.1	513.03	290.000	3484.0	511.74	290.000	2998.9	510.56
290.000	2510.0	509.33	290.000	2004.4	508.04	290.000	1499.4	506.71
300.000	7004.4	506.54	300.000	6496.7	505.29	300.000	6063.5	504.20
300.000	5518.9	502.75	300.000	4937.0	501.23	300.000	4462.1	499.91
300.000	4036.8	498.73	300.000	3486.3	497.18	300.000	3032.3	495.86
300.000	2519.2	494.32	300.000	2015.2	492.77	300.000	1517.7	491.19
300.000	997.6	489.48[a]	310.000	6991.8	492.41	310.000	6510.1	491.02
310.000	6046.3	489.64	310.000	5529.3	488.08	310.000	5029.4	486.52
310.000	4528.9	484.91	310.000	4040.6	483.29	310.000	3515.0	481.48
310.000	3012.9	479.70	310.000	2491.2	477.78	310.000	2018.8	475.98
310.000	1514.4	473.96	310.000	1272.1	472.96[a]	320.000	7008.9	477.63
320.000	6523.4	475.95	320.000	6024.8	474.19	320.000	5536.8	472.40
320.000	5017.9	470.44	320.000	4519.6	468.46	320.000	4025.8	466.44
320.000	3495.1	464.17	320.000	3002.1	461.96	320.000	2513.8	459.66
320.000	2011.4	457.17	320.000	1600.7	455.00[a]	330.000	6985.1	461.52
330.000	6499.8	459.50	330.000	6010.6	457.38	330.000	5488.6	455.01
330.000	4996.1	452.66	330.000	4495.8	450.17	330.000	3995.4	447.53
330.000	3909.1	447.05	330.000	3546.3	445.00	330.000	3032.0	441.91
330.000	2537.4	438.74	330.000	2033.9	435.23	330.000	1988.8	434.90[a]
340.000	6964.1	444.10	340.000	6494.7	441.64	340.000	5985.0	438.83
340.000	5516.7	436.10	340.000	5027.1	433.06	340.000	4501.8	429.56
340.000	4014.0	426.05	340.000	3507.8	422.07	340.000	3024.2	417.87
340.000	2429.7	411.92[a]	350.000	6978.1	424.88	350.000	6491.4	421.59
350.000	6027.1	418.22	350.000	5521.6	414.24	350.000	5024.8	409.94
350.000	4505.9	404.94	350.000	4011.9	399.51	350.000	3541.2	393.49
350.000	2948.0	384.39[a]	360.000	6953.8	402.50	360.000	6529.9	398.56
360.000	6048.5	393.63	360.000	5524.7	387.51	360.000	5043.0	380.99
360.000	4527.8	372.52	360.000	4043.5	362.08	360.000	3552.2	347.97[a]
370.000	2783.7	55.36[b]	370.000	2081.6	37.08[b]	370.000	1515.9	25.15[b]
370.000	1089.1	17.21[b]	370.000	779.8	11.91[b]	370.000	4325.4	287.46
370.000	7066.4	377.66	370.000	6504.8	369.98	370.000	5998.0	361.65
370.000	5527.4	352.01	370.000	4996.9	336.94	370.000	4521.7	312.65
380.000	7012.1	344.89	380.000	6541.5	333.99	380.000	6044.5	318.37
380.000	5530.3	291.64	380.000	5335.4	273.87	380.000	4556.5	131.82[b]
380.000	4060.6	97.22[b]	380.000	4059.9	97.18[b]	380.000	4059.0	97.16[b]
380.000	3340.1	67.96[b]	380.000	2630.4	47.90[b]	380.000	2032.0	34.39[b]
380.000	1564.3	25.22[b]	380.000	1223.8	19.12[b]	380.000	813.8	12.27[b]

[a] Datum in the saturated liquid phase. [b] Datum in the supercritical state.

Materials. We have used research-grade samples of propane, *n*-butane, and isobutane with a purity of 99.99 mol %. This purity information was provided by the chemical manufacturer, Nippon Sanso Co., and we did not conduct any further purification except degassing.

Results and Discussion

A total of 192, 128, and 110 *PVT* properties were obtained for propane, *n*-butane, and isobutane, respectively. These data widely range from (240 to 380) K, up to 7 MPa, in the liquid phase including data along the saturation curves. Tables 1, 2, and 3 tabulate the present measured data. Figures 3, 4, and 5 illustrate the distribution of the present data for propane, *n*-butane, and isobutane on a $P-T$ diagram, respectively. Available *PVT* property data are also plotted in the diagrams. Concerning *n*-butane and isobutane, it is recognized that the present measurements are the first data reported since the piezometric measurements by Kay,[9] Olds et al.,[10] Morris et al.,[11] and Sage and Lacey[12] published around 1940.

Table 2. Experimental *PVT* Data for *n*-Butane

T/K	P/kPa	ρ/kg·m^{-3}	T/K	P/kPa	ρ/kg·m^{-3}	T/K	P/kPa	ρ/kg·m^{-3}
240.000	26.2	634.72[a]	240.000	23.9	634.79[a]	240.000	7115.6	642.22
240.000	6517.3	641.67	240.000	5990.8	641.21	240.000	5540.8	640.78
240.000	5029.0	640.31	240.000	4487.8	639.80	240.000	4001.2	639.35
240.000	3512.2	638.87	240.000	3029.5	638.41	240.000	2570.2	637.97
240.000	2000.1	637.42	240.000	1510.1	636.95	240.000	1007.3	636.47
240.000	486.0	635.96	260.000	59.9	615.48[a]	260.000	6989.2	623.08
260.000	6478.7	622.54	260.000	6003.3	622.01	260.000	5503.1	621.46
260.000	5004.2	620.91	260.000	4494.6	620.36	260.000	3997.0	619.80
260.000	3506.9	619.26	260.000	3039.4	618.72	260.000	2488.3	618.09
260.000	2020.3	617.55	260.000	1521.8	616.98	260.000	998.4	616.36
260.000	481.0	615.74	280.000	131.5	593.89[a]	280.000	7020.0	603.37
280.000	6499.1	602.71	280.000	5929.2	601.98	280.000	5428.9	601.30
280.000	4975.0	600.69	280.000	4513.6	600.07	280.000	3974.9	599.34
280.000	3516.7	598.71	280.000	2985.5	597.98	280.000	2465.8	597.26
280.000	1987.6	596.59	280.000	1472.7	595.86	280.000	992.0	595.16
280.000	493.9	594.44	280.000	173.2	593.97	280.000	144.7	593.92
300.000	256.4	571.03[a]	300.000	7089.3	582.62	300.000	6459.3	581.65
300.000	5951.1	580.88	300.000	5543.6	580.23	300.000	4990.4	579.31
300.000	4525.1	578.55	300.000	3992.8	577.66	300.000	3499.9	576.83
300.000	2964.0	575.92	300.000	2499.1	575.12	300.000	2013.4	574.26
300.000	1491.3	573.35	300.000	992.8	572.45	300.000	493.4	571.55
300.000	315.1	571.23	300.000	268.9	571.14	320.000	6982.1	560.62
320.000	6510.5	559.67	320.000	6031.0	558.74	320.000	5473.8	557.60
320.000	4992.8	556.63	320.000	4513.3	555.64	320.000	4015.6	554.60
320.000	4017.2	554.60	320.000	3523.1	553.55	320.000	3010.6	552.45
320.000	2517.1	551.36	320.000	2011.8	550.22	320.000	1502.7	549.06
320.000	1002.9	547.89	320.000	515.9	546.74	320.000	454.8	546.56[a]
340.000	750.5	520.07[a]	340.000	751.0	519.84[a]	340.000	7014.5	537.36
340.000	6451.2	535.97	340.000	5975.4	534.78	340.000	5471.0	533.51
340.000	4964.4	532.19	340.000	4437.7	530.79	340.000	4034.7	529.70
340.000	3504.4	528.23	340.000	3012.7	526.82	340.000	2514.4	525.36
340.000	1975.7	523.74	340.000	1519.5	522.33	340.000	989.9	520.64
340.000	791.7	519.97	340.000	761.5	519.87	360.000	1168.5	490.27[a]
360.000	7012.4	512.64	360.000	6486.7	510.96	360.000	5979.4	509.32
360.000	5504.8	507.65	360.000	4984.1	505.83	360.000	4488.7	504.06
360.000	3993.1	502.23	360.000	3489.7	500.29	360.000	2995.1	498.32
360.000	2493.7	496.23	360.000	2006.4	494.12	360.000	1507.5	491.85
360.000	1215.8	490.48	360.000	1181.7	490.31	360.000	1168.1	490.24[a]
380.000	6978.0	484.82	380.000	6534.9	482.88	380.000	6013.8	480.51
380.000	5511.1	478.12	380.000	5015.7	475.66	380.000	4508.9	473.00
380.000	3999.9	470.18	380.000	3502.0	467.25	380.000	3010.6	464.17
380.000	2503.7	460.77	380.000	2007.2	457.14	380.000	1925.7	456.51
380.000	1845.2	455.88	380.000	1737.4	455.00[a]			

[a] Datum in the saturated liquid phase.

First, the liquid-phase *PVT* properties were compared with a set of equations of state for HC refrigerants formulated by Miyamoto and Watanabe[1−3] (MWEoS hereafter). These equations of state are adopted in REFPROP,[4] the thermodynamic-property calculation software. The relative density deviation of the present liquid-phase data from the EoS was shown in Figures 6, 7, and 8, together with those for available liquid-phase *PVT* data.

Concerning the deviation plot for propane shown in Figure 6, the present experimental data agree well with MWEoS within ±0.1% at lower temperatures from (240 to 290) K. The relative density deviation slightly increases at higher temperatures but still falls within ±0.4% even near the critical temperature (i.e., 369.811 K[13]). The "S"-shaped systematic deviation of ±0.2% is observed for the present data. Accordingly, it is considered that the *PVT* surface of the MWEoS may be slightly bent as a result of fitting to a number of experimental data with a large uncertainty.

From Figure 7, it is found that the present liquid-density data have a certain bias from those predicted by the MWEoS with a maximum departure of 0.3 at 380 K. Those reported at lower temperatures by Haynes[14] are confirmed

Table 3. Experimental *PVT* Data for Isobutane

T/K	P/kPa	ρ/kg·m^{-3}	T/K	P/kPa	ρ/kg·m^{-3}	T/K	P/kPa	ρ/kg·m^{-3}
240.000	40.1	617.17[a]	240.000	7010.9	624.66	240.000	6540.8	624.19
240.000	5987.3	623.62	240.000	5522.1	623.14	240.000	5022.8	622.62
240.000	4542.1	622.10	240.000	4038.4	621.58	240.000	3501.9	621.00
240.000	3029.3	620.49	240.000	2522.8	619.95	240.000	2037.8	619.41
240.000	1538.4	618.86	240.000	1027.4	618.30	240.000	484.1	617.68
260.000	94.6	595.32[a]	260.000	7031.7	604.37	260.000	6532.0	603.75
260.000	5953.7	603.05	260.000	5481.6	602.44	260.000	4915.7	601.73
260.000	4464.7	601.16	260.000	4015.9	600.60	260.000	3472.2	599.90
260.000	3005.3	599.28	260.000	2532.0	598.66	260.000	1984.7	597.94
260.000	1503.8	597.28	260.000	947.4	596.52	260.000	517.1	595.93
280.000	197.8	572.74[a]	280.000	6980.4	583.64	280.000	6507.2	582.93
280.000	5986.9	582.16	280.000	5494.5	581.39	280.000	4938.8	580.54
280.000	4460.5	579.80	280.000	4015.2	579.09	280.000	3506.0	578.27
280.000	2999.4	577.44	280.000	2508.1	576.64	280.000	2000.6	575.80
280.000	1532.9	575.01	280.000	996.0	574.10	280.000	512.2	573.26
300.000	368.6	548.27[a]	300.000	7025.2	561.79	300.000	6460.3	560.72
300.000	5953.2	559.79	300.000	5467.8	558.87	300.000	4980.2	557.93
300.000	4482.8	556.96	300.000	3965.8	555.93	300.000	3526.2	555.05
300.000	3021.3	554.01	300.000	2533.3	552.99	300.000	1999.9	551.86
300.000	1462.4	550.70	300.000	1017.6	549.71	300.000	476.5	548.51
320.000	632.5	521.48[a]	320.000	6995.3	538.27	320.000	6511.5	537.15
320.000	5960.5	535.86	320.000	5450.3	534.62	320.000	4946.7	533.39
320.000	4496.4	532.26	320.000	4027.5	531.05	320.000	3521.6	529.72
320.000	3037.4	528.43	320.000	2548.7	527.08	320.000	2072.9	525.74
320.000	1503.5	524.10	320.000	1063.0	522.78	340.000	1013.7	491.87[a]
340.000	6962.7	513.39	340.000	6512.9	512.03	340.000	5998.3	510.42
340.000	5520.7	508.89	340.000	5017.1	507.23	340.000	4507.3	505.51
340.000	4023.8	503.83	340.000	3503.8	501.94	340.000	3002.8	500.07
340.000	2499.6	498.13	340.000	2007.1	496.16	340.000	1494.6	493.98
360.000	1541.6	457.33[a]	360.000	6987.7	486.08	360.000	6485.4	484.01
360.000	6006.8	481.96	360.000	5482.2	479.63	360.000	5024.7	477.51
360.000	4532.2	475.11	360.000	4027.6	472.55	360.000	3502.9	469.71
360.000	2997.5	466.82	360.000	2503.6	463.81	360.000	2008.5	460.57
380.000	2250.4	413.34[a]	380.000	6952.1	454.64	380.000	6503.3	451.96
380.000	6019.7	448.91	380.000	5519.1	445.53	380.000	4990.6	441.69
380.000	4487.2	437.71	380.000	4014.9	433.63	380.000	3511.0	428.79
380.000	3027.5	423.54	380.000	2517.9	417.11			

[a] Datum at the saturated liquid phase.

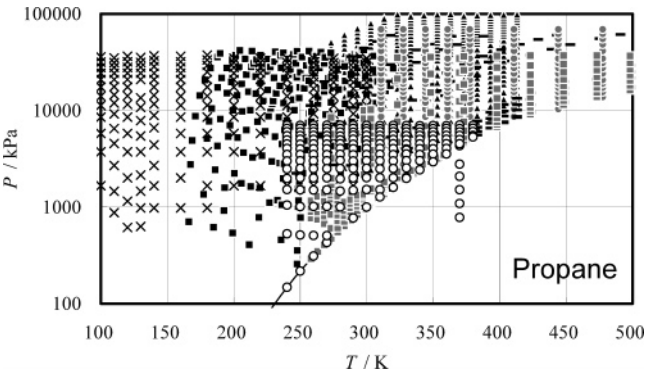

Figure 3. *PVT* data distribution for propane: ○, this work; ▲, Dittmar et al.;[23] ■, Ely and Kobayashi;[21] ×, Haynes;[20] −, Kratzke and Mueller;[24] ● (in gray), Reamer et al.;[25] ■ (in gray), Thomas and Harrison.[26]

to be set in ±0.15% from the baseline. Although there are slight fluctuations for liquid-density data by Beattie,[15] Kay,[9] and Olds et al.,[10] it is considered that those data satisfactorily agree with the baseline as long as the date of measurements of these data around the 1940s is considered.

It was also found from Figure 8 that the present liquid-density data show an S-shaped systematic deviation from the MWEoS. The density difference becomes large at higher temperatures to a maximum of 0.4%. At temperatures of (300 to 380) K, there are no data other than piezometry data by Morris et al.,[11] Sage and Lacey,[12] and our data. Therefore, it is considered to be unreasonable to require high reproducibility to the EoS. It may also be said that the present data provide important information about liquid-phase *PVT* properties for isobutane.

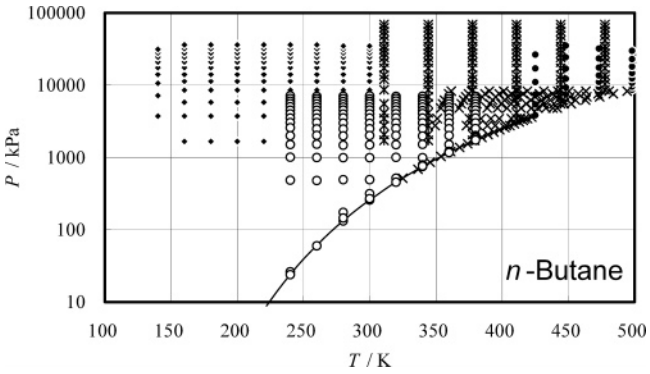

Figure 4. *PVT* data distribution for *n*-butane: ○, this work; ●, Beattie et al.;[15] ◆, Haynes;[14] ×, Kay;[9] *, Olds et al.[10]

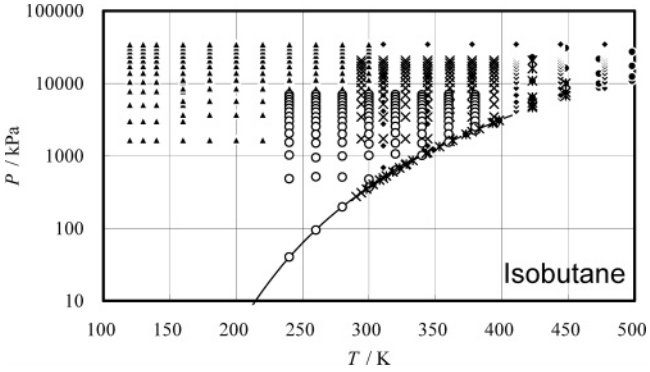

Figure 5. *PVT* data distribution for isobutane: ○, this work; ●, Beattie et al.;[27] ▲, Haynes;[22] ◆, Morris et al.;[11] ×, Sage and Lacey;[12] *, Waxman et al.[28]

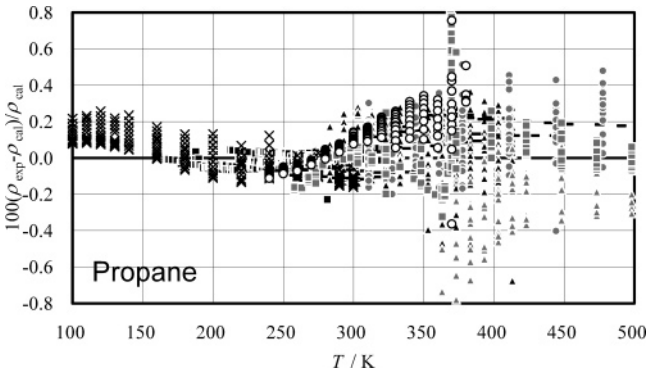

Figure 6. Relative density deviation of the liquid-density data for propane from the Miyamoto and Watanabe EoS:[1] ○, this work; ▲, Dittmar et al.;[23] ■, Ely and Kobayashi;[21] ×, Haynes;[20] −, Kratzke and Mueller;[24] ● (in gray), Reamer et al.;[25] ▲ (in gray), Straty and Palavra;[29] ■ (in gray), Thomas and Harrison;[26] ◆ (in gray), Warowny et al.[30]

In the present study, vapor pressures for propane, *n*-butane, and isobutane were also measured in the temperature range from 240 K to 380 K or the critical temperature for propane. These data and available literature data were also compared with the MWEoS in Figures 9, 10, and 11, respectively.

From Figure 9, it is found that most of the present data agree well with the MWEoS within a scatter of ±3 kPa. The vapor-pressure data for *n*-butane obtained in the present study have a similar negative deviation of about −3.5 kPa maximum. Concerning the present vapor-pressure data for isobutane, it was found that they were well reproduced by the MWEoS only within ±1.5 kPa. The available vapor-pressures for isobutane have relatively large scatter of ±10 KPa. Hence, it can be said that the

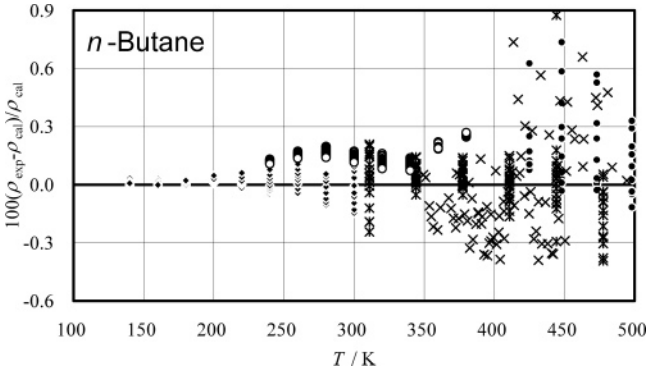

Figure 7. Relative density deviation of the liquid-density data for *n*-butane from the Miyamoto and Watanabe EoS:[2] ○, this work; ●, Beattie et al.;[15] ▲, Haynes;[14] ×, Kay;[9] *, Olds et al.[10]

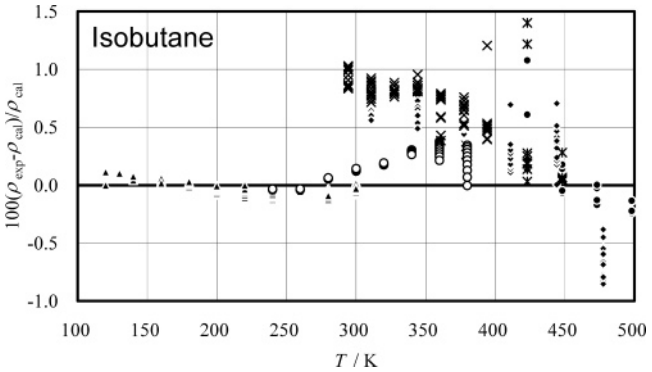

Figure 8. Relative density deviation of the liquid-density data for isobutane from the Miyamoto and Watanabe EoS:[3] ○, this work; ●, Beattie et al.;[27] ▲, Haynes;[22] ◆, Morris et al.;[11] ×, Sage and Lacey;[12] *, Waxman et al.[28]

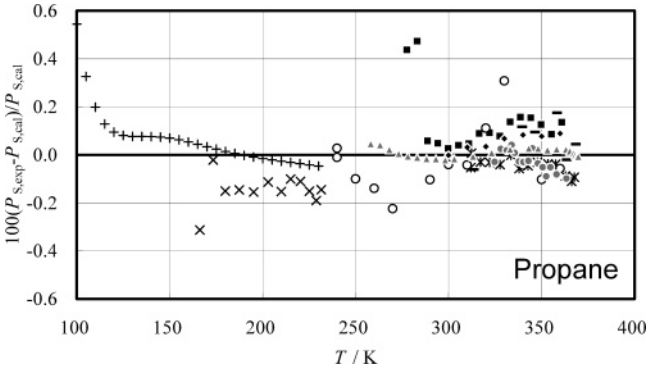

Figure 9. Relative deviation of the vapor-pressure data for propane from the Miyamoto and Watanabe EoS:[1] ○, this work; ■, Helgeson and Sage;[31] ◆, Hondo et al.;[32] ×, Kemp and Egan;[33] *, Kratzke;[34] +, Magee;[35] −, Reamer et al.;[25] ● (in gray), Teichmann;[36] ▲ (in gray), Thomas and Harrison.[26]

soundness of the prediction of the MWEoS for isobutane was confirmed by the present measurements.

The saturated liquid densities for propane, *n*-butane, and isobutane were also compared with the MWEoS in Figures 12, 13, and 14, respectively.

Excellent agreement of the present data with the MWEoS appears in Figure 12. In the temperature range below 350 K, it is confirmed that all of the data obtained in the present study agree well with the EoS within ±0.1%. At higher temperatures, the data deviate to 0.6%, as do other reported data, because they are close to the critical temperature.

Concerning the saturated liquid densities for *n*-butane, the present data have a positive systematic deviation by

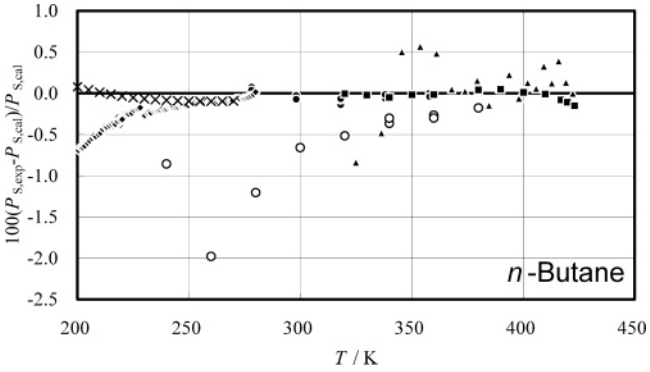

Figure 10. Relative deviation of the vapor-pressure data for *n*-butane from the Miyamoto and Watanabe EoS:[2] ○, this work; ●, Flebbe et al.;[37] ▲, Kay;[9] ■, Kratzke;[34] ◆, Machin and Golding;[38] ×, Magee.[35]

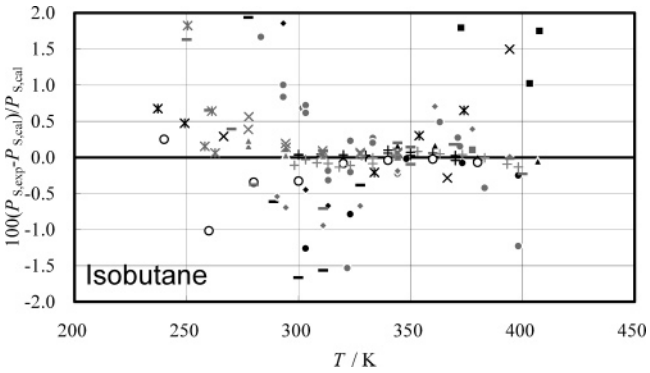

Figure 11. Relative deviation of the vapor-pressure data for isobutane from the Miyamoto and Watanabe EoS:[3] ○, this work; ●, Beattie et al.;[39] ▲, Connolly;[40] ■, Gilliland and Scheeline;[41] ◆, Higashi et al.;[42] ×, Hipkin;[43] *, Hirata and Suda;[44] +, Hondo et al.;[32] −, Kahre;[45] ● (in gray), KIST;[46–50] ▲ (in gray), Martinez-Ortiz and Manley;[51] ■ (in gray), Morris et al.;[11] ◆ (in gray), Sage and Lacey;[12] × Steele et al.;[52] * (in gray), Wackher et al.;[53] + (in gray), Waxman et al.;[28] − (in gray), Weber.[54–56]

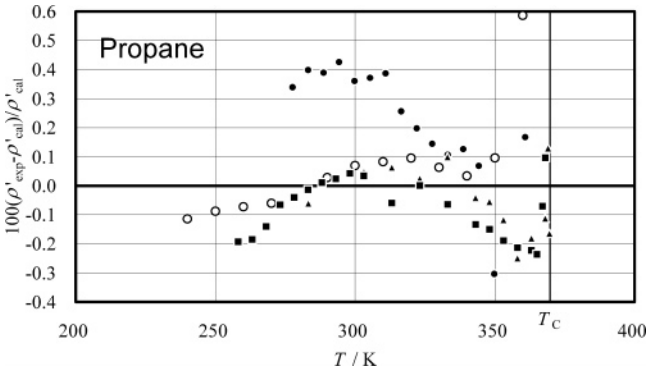

Figure 12. Relative deviation of the saturated-liquid density data for propane from the Miyamoto and Watanabe EoS:[1] ○, this work; ●, Helgeson and Sage;[31] ▲, Sliwinski;[57] ■, Thomas and Harison.[26]

about +0.07% to +0.26% from the baseline. This trend is different from those for the majority of the available data by Haynes,[14] Orrit and Laupretre,[16] and Sliwinski.[17]

From Figure 14, the present data were found to have a systematic deviation from the prediction of the MWEoS, but they are still within ±0.3%. It is interesting that this behavior is similar to that for the data by Sliwinski.[17]

Liquid-Density Equation

To represent the thermodynamic properties in the liquid phase of propane, *n*-butane, and isobutane obtained in the

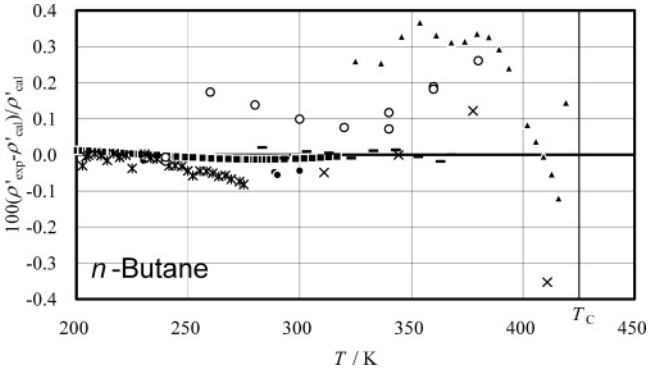

Figure 13. Relative deviation of the saturated-liquid density data for *n*-butane from the Miyamoto and Watanabe EoS:[2] ○, this work; ●, Haynes;[14] ▲, Kay;[9] ■, Magee;[35] ×, Olds et al.;[10] *, Orrit and Laupretre;[16] −, Sliwinski.[17]

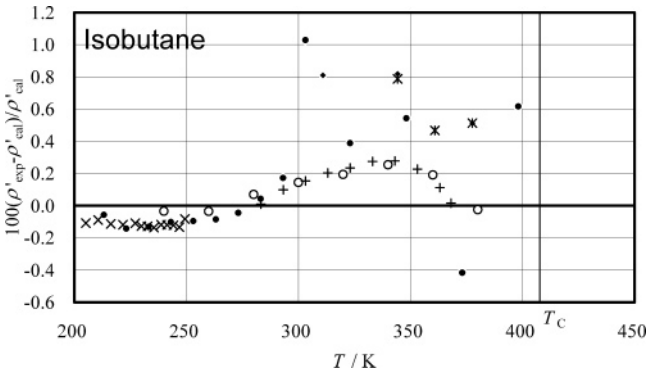

Figure 14. Relative deviation of the saturated-liquid density data for isobutane from the Miyamoto and Watanabe EoS:[3] ○, this work; ●, Beattie et al.;[39] ◆, Morris et al.;[11] ×, Orrit and Laupretre;[16] *, Sage and Lacey;[12] +, Sliwinski.[17]

present study, we have developed an empirical equation of state. The original basic function of the EoS was proposed by Sato[18] to represent the thermodynamic properties of water as a modified form of the van der Waals equation of state. We have employed this basic function to represent the liquid-phase thermodynamic properties for light hydrocarbons. The functional form of the EoS is given by

$$\rho_r = \frac{(P_r + A(T_r))^{C(T_r)}}{D(T_r)} \tag{8}$$

$$A(T) = \sum_{k=0}^{2} a_i T_r^{\,k} \tag{9}$$

$$C(T) = \sum_{k=0}^{2} c_i T_r^{\,k} \tag{10}$$

$$D(T) = \sum_{k=0}^{2} d_i T_r^{\,k} \tag{11}$$

T_r, P_r, and ρ_r are the reduced temperature, pressure, and density, respectively. They are nondimensionalized by the critical parameters (e.g., $T_r = T/T_C$). As for the critical parameters for propane and isobutane used in the present EoS, we have employed those reported by Yoshii.[13] As for *n*-butane, those by Haynes and Goodwin[19] were employed. It should be noted that the critical pressure values for propane and isobutane were originally optimized from the vapor-pressure correlation. These parameters are summarized in Table 4.

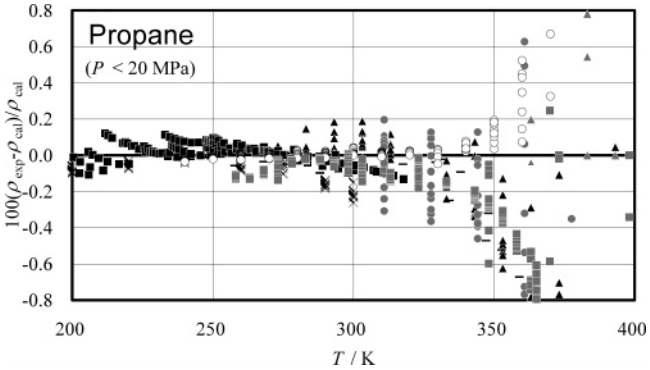

Figure 15. Relative density deviation of the liquid-density data for propane from eq 8: ○, this work; ▲, Dittmar et al.;[23] ■, Ely and Kobayashi;[21] ×, Haynes;[20] −, Kratzke and Mueller;[24] ● (in gray), Reamer et al.;[25] ▲ (in gray), Straty and Palavra;[29] ■ (in gray), Thomas and Harrison;[26] ◆ (in gray), Warowny et al.[30]

Table 4. Numerical Constants for Equations 8−11

substance	propane	*n*-butane	isobutane
T_C/K	369.811	425.125	407.761
P_C/kPa	4248	3796	3631
ρ_C/kg·m^{-3}	222	227.84	233
a_0	51.5282	39.0313	40.0811
a_1	−90.2975	−63.6158	−66.0010
a_2	37.8007	23.5672	24.9675
c_0	0.102351	0.072934	0.077124
c_1	−0.077820	−0.075024	−0.078421
c_2	0.087578	0.109702	0.113271
d_0	0.404740	0.352283	0.369925
d_1	0	−0.000028	−0.000241
d_2	0.160565	0.208062	0.213270

This equation of state is valid in the liquid phase; however, the temperature range is up to the reduced temperature, $T_r = 0.95$, where the isothermal compressibility moderately changes. At higher temperatures, the EoS may not be effective because of the steep curvature of the $P-\rho$ isotherm.

In the present study, numerical constants a_0 through d_2 were determined by a nonlinear regression of the EoS to the present data obtained by the vibrating-tube densimeter apparatus. Concerning the input data for propane, we did not use data at temperatures higher than $T_r = 0.95$. Thus-determined numerical constants are summarized in Table 4.

Concerning the valid range of the EoS that was fitted to the present data for (240 to 380) K, up to 7 MPa, it is expected to be valid down to 200 K. However, the pressure limit of the present EoS for the liquid phase is not strictly restricted by the input data range, but it is expected to be effective at pressures up to 20 MPa.

The relative density deviation of the reported data at pressures up to 20 MPa from eq 8 is illustrated in Figure 15. The EoS is in good agreement with the present data within ±0.08% at temperatures up to 340 K. As the temperature rises, the deviation increases to 0.5%. It is found from Figure 15 that eq 8 represents the reported liquid-density data with good reproducibility. The maximum deviation of the data for temperatures between 240 K and 350 K is less than ±0.2%. Equation 8 has the best reproducibility among the available representations at lower temperatures from 210 K to 290 K, although all of them agree well with eq 8 within ±0.15%. The data at lower temperatures down to 100 K reported by Haynes[20] and by Ely and Kobayashi[21] have slight systematic devia-

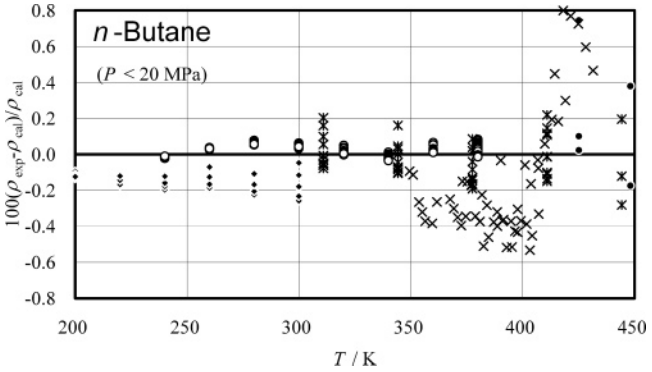

Figure 16. Relative density deviation of the liquid-density data for *n*-butane from eq 8: ○, this work; ●, Beattie et al.;[15] ◆, Haynes;[14] ×, Kay;[9] *, Olds et al.[10]

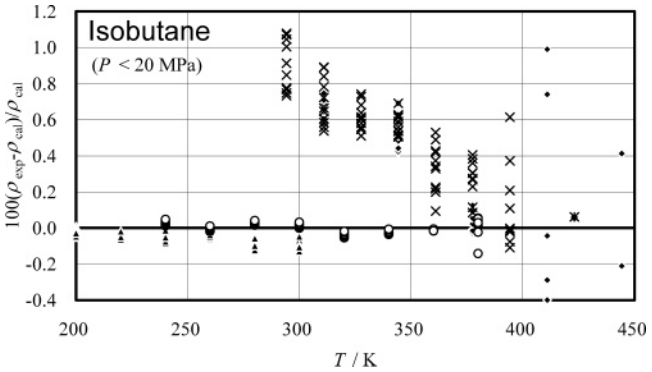

Figure 17. Relative density deviation of the liquid-density data for isobutane from eq 8: ○, this work; ●, Beattie et al.;[27] ▲, Haynes;[22] ◆, Morris et al.;[11] ×, Sage and Lacey;[12] *, Waxman et al.[28]

tions, but they are not greater than −1.0% even at 120 K. Although the reproducibility of eq 8 also decreases in the vicinity of the critical point, all of the data are reproduced within ±1.0% at temperatures up to 360 K. Judging from these facts, the lowest-temperature limit for eq 8 to be valid is expected to be down to 200 K, whereas the highest-temperature limit is about 360 K because of the effectiveness of the EoS.

Figure 16 illustrates the relative density deviation of the present data and other reported density data for *n*-butane from those calculated by eq 8. The reported data above 20 MPa were not included in Figure 16 for the same reason as that discussed previously. From the deviation plot, it is apparent that eq 8 excellently represents the input data obtained in the present study within ±0.06%. Equation 8 also shows a good representation for liquid-density data by Haynes[14] within ±0.15%. As already discussed above, other reported data have a relatively wider scatter from the baseline. However, this fact is considered to be acceptable by considering the measurement uncertainty of these data.

A similar comparison was made for isobutane, as shown in Figure 17. The present data were confirmed to agree with the baseline EoS, eq 8, excellently within ±0.05% except for a single datum at 380 K. To examine the extrapolation capability of eq 8 with respect to temperature, it is compared with the available liquid-density data at pressures up to 20 MPa. It is found that eq 8 has good reproducibility within ±0.3% of the data by Haynes[22] down to 200 K. As for temperatures between 310 K and 350 K, all of the data including those by Haynes and those by Sage and Lacey[12] deviate by about +0.5% to +1.0% from eq 8. The temperature behavior of the data by Haynes shows a

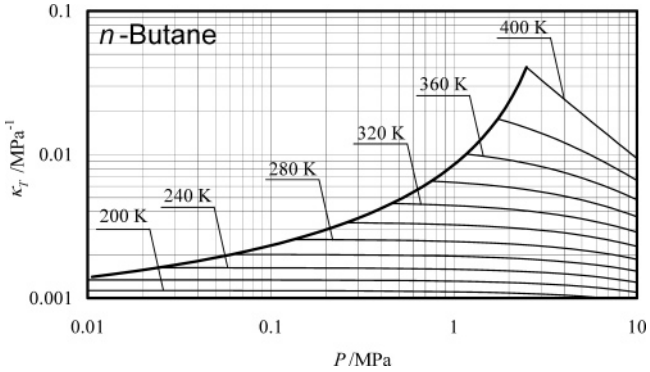

Figure 18. Pressure dependence of the isothermal compressibility for *n*-butane derived from eq 8.

certain discrepancy at temperatures between 300 K and 310 K, which is considered to be inconsistent. Regarding this temperature range, it is considered that some unknown thermodynamic behavior of isobutane may exhibit this gap. Further investigation regarding this issue is expected to be done. Although the issue that a considerable observed discrepancy for the data at temperatures between 310 K and 350 K remains unsolved, eq 8 has satisfactory effectiveness for temperatures from 200 K to 400 K and pressures up to 20 MPa.

To confirm the thermodynamic consistency of eq 8, we derived properties such as the isochoric heat capacity, c_v, isobaric heat capacity, c_P, speed of sound, w, and isothermal compressibility, κ_T from eq 8. These properties were evaluated by applying following thermodynamic relations.

$$c_v = c_P + \frac{T\left(\frac{\partial v}{\partial T}\right)_P^2}{\rho^2\left(\frac{\partial v}{\partial P}\right)_T} \tag{12}$$

$$c_P = c_P' - \int_{P_S}^{P} T\left(\frac{\partial^2 v}{\partial T^2}\right)_P \mathrm{d}P \tag{13}$$

$$w = \sqrt{\frac{c_P}{\rho\alpha_T c_v}} \tag{14}$$

$$\kappa_T = \frac{C}{A+P} \tag{15}$$

In the present paper, these properties for *n*-butane are discussed as an example because the behavior of these properties calculated from the present EoS is not very different from each other.

In eq 13, c_P' denotes the saturated-liquid isobaric heat capacity. To calculate these derived properties, the computed c_P' values were employed as the reference state. Figures 18, 19, and 20 illustrate the pressure dependences of the isothermal compressibility, isobaric heat capacity, and speed of sound for *n*-butane, respectively.

It is recognized from these Figures that eq 8 can yield a thermodynamically sound property surface within its valid temperature range (from 200 K to 409 K = $0.95T_C$). As for the same examination of eq 8 for propane, unreasonable behavior of the isochoric heat capacity was observed for an isotherm of 360 K. Because that temperature (T_r = 0.973) is very close to the critical point and is not valid for eq 8, the thermodynamic consistency would be lost in this temperature range. At temperatures below $T_r = 0.95$, the

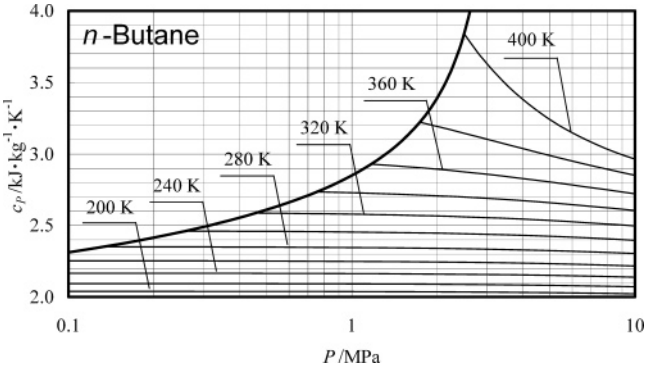

Figure 19. Pressure dependence of the isobaric heat capacity for *n*-butane derived from eq 8.

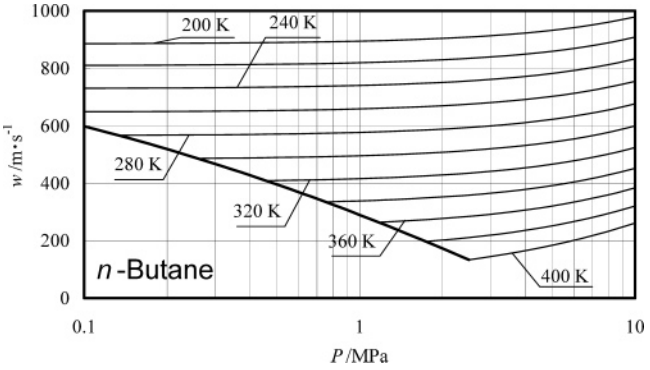

Figure 20. Pressure dependence of the speed of sound for *n*-butane derived from eq 8.

present EoS is confirmed to be reasonable by examining the behavior of these derived properties.

Conclusions

Hydrocarbon refrigerants are expected to be promising alternatives for halogenated hydrocarbon refrigerants that have a large global warming potential. Equations of state (EoS) for these three hydrocarbons have recently been updated but are still based on relatively old measured data. In the present study, a total of 192, 128, and 110 liquid *PVT* properties were obtained for propane, *n*-butane, and isobutane, respectively. From the comparison of these data with the EoS, a slight systematic density deviation was found. Further accurate measurements for *PVT* properties are expected in order to develop reliable thermodynamic models for these hydrocarbons. A modified Tait EoS proposed by Sato in 1981 was applied to correlate the present data. The EoS was exclusively fitted to the present data, and it represents these input data excellently within ±0.1% as far as its effective range (i.e., 200 K to $0.95T_C$) up to 20 MPa. The thermodynamic property surface of the EoS was examined in terms of essential derived properties such as heat capacities, speed of sound, and isothermal compressibility.

Acknowledgment

We are gratefull to Dr. Hiroyuki Miyamoto for his kind help with his database of the experimental data for hydrocarbons. This study was supported by a Grant-in-Aid from the Scientific Research Fund from 2000 to 2002 (project no.12450090), Ministry of Education, Culture, Sports, Science and Technology, Japan.

Literature Cited

(1) Miyamoto, H.; Watanabe, K. A Thermodynamic Property Model for Fluid-Phase Propane. *Int. J. Thermophys.* **2000**, *21*, 1045−1072.
(2) Miyamoto, H.; Watanabe, K. A Thermodynamic Property Model for Fluid-Phase *n*-Butane. *Int. J. Thermophys.* **2001**, *22*, 459−475.
(3) Miyamoto, H.; Watanabe, K. A Thermodynamic Property Model for Fluid-Phase Isobutane. *Int. J. Thermophys.* **2002**, *23*, 477−499.
(4) Lemmon, E. W.; McLlinden, M. O.; Huber, M. L. *REFPROP, Reference Fluid Thermodynamic and Transport Properties*; NIST Standard Reference Database 23, version 7.0; National Institute of Standards and Technology, U.S. Department Commerce: Washington, DC, 2002.
(5) Younglove, B. A.; Ely, J. F. Thermophysical Properties of Fluids. II. Methane, Ethane, Propane, Isobutane and Normal Butane. *J. Phys. Chem. Ref. Data*. **1987**, *16*, 577−798.
(6) Kayukawa, Y.; Hasumoto, M.; Watanabe, K. Rapid Density-Measurement System with Vibrating Tube Densimeter. *Rev. Sci. Instrum.* **2003**, *74*, 4134−4139.
(7) Kayukawa, Y. A Study of Thermodynamic Properties for Novel Refrigerants with Rapid and Precise Density Measurement Technique. Ph.D. Thesis, Keio University, Yokohama, Japan, 2002.
(8) *Guide to the Expression of Uncertainty in Measurement*; International Organization of Standardization (ISO): Switzerland, 1993; p 101
(9) Kay, W. B. Pressure−Volume−Temperature Relations for *n*-Butane. *Ind. Eng. Chem.* **1940**, *32*, 358−360.
(10) Olds, R. H.; Reamer, H. H.; Sage, B. H.; Lacey, W. N. Phase Equilibria in Hydrocarbon Systems, Volumetric Behavior of *n*-Butane. *Ind. Eng. Chem.* **1944**, *36*, 282−284.
(11) Morris, W. M.; Sage, B. H.; Lacey, W. N. Technical Publication 1128; National Bureau of Standards: 1939.
(12) Sage, B. H.; Lacey, W. N. Phase Equilibrium in Hydrocarbon Systems, Thermodynamic Properties of Isobutane. *Ind. Eng. Chem.* **1938**, *30*, 673−681.
(13) Yoshii, Y. Measurements of Saturation Densities and Critical Parameters for Alternative Refrigerants with Less Environmental Impact (in Japanese). Master's Thesis, Keio University, Yokohama, Japan, 2001.
(14) Haynes, W. M. Measurements of Densities and Dielectric Constants of Liquid Normal Butane from 140 to 300 K at Pressures to 35 MPa. *J. Chem. Thermodyn.* **1983**, *15*, 801−805.
(15) Beattie, J. A.; Simard, G. L.; Su, G.-J. The Vapour Pressure and Critical Constants of Normal Butane. *J. Am. Chem. Soc.* **1939**, *61*, 24−26.
(16) Orrit, J. E.; Laupretre, J. M. Density of Liquefied Natural Gas Components. *Adv. Cryog. Eng.* **1978**, *23*, 573−579.
(17) Sliwinski, P. Die Lorentz−Lorenz-Funktion von Dampfförmigem und Flüssigem Äthan, Propan und Butan. *Z. Phys. Chem. Neue. Folge.* **1969**, *68*, 263−279.
(18) Sato, H. A Study on Thermodynamic Property Surface of Water and Steam under High Pressures (in Japanese). Ph.D. Thesis, Keio University, Yokohama, Japan, 1981.
(19) Haynes, W. M.; Goodwin, R. D. *Thermophysical Properties of Normal Butane from 135 to 700 K at Pressures to 70 MPa*; NBS Monograph 169; National Bureau of Standards: 1982.
(20) Haynes, W. M. Measurements of Densities and Dielectric Constants of Liquid Propane from 90 to 300 K at Pressures to 35 MPa. *J. Chem. Thermodyn.* **1983**, *15*, 419−424.
(21) Ely, J. F.; Kobayashi, R. Isochoric Pressure−Volume−Temperature Measurements for Compressed Liquid Propane. *J. Chem. Eng. Data*. **1978**, *23*, 221−223.
(22) Haynes, W. M. Measurements of Densities and Dielectric Constants of Liquid Isobutane from 130 to 300 K at Pressures to 35 MPa. *J. Chem. Eng. Data* **1983**, *28*, 367−369.
(23) Dittmar, P.; Schulz, F.; Strese, G. Druck/Dichte/Temperatur-Werte für Propan und Propylen. *Chem.-Ing.-Tech.* **1962**, *34*, 437−441.
(24) Kratzke, H.; Müller, S. Thermodynamic Quantities for Propane, 3. The Thermodynamic Behavior of Saturated and Compressed Liquid Propane. *J. Chem. Thermodyn.* **1984**, *16*, 1157−1174.
(25) Reamer, H. H.; Sage, B. H.; Lacey, W. N. Phase Equilibria in Hydrocarbon Systems, Volumetric Behavior of Propane. *Ind. Eng. Chem.* **1949**, *41*, 482−484.
(26) Thomas, R. H. P.; Harrison, R. H. Pressure−Volume−Temperature Relations of Propane. *J. Chem. Eng. Data*. **1982**, *27*, 1−11.
(27) Beattie, J. A.; Marple, S., Jr.; Edwards, D. G. The Compressibility of, and an Equation of State for Gaseous Isobutane. *J. Chem. Phys.* **1950**, *18*, 127−128.
(28) Waxman, M.; Davis, H. A.; Levelt Sengers, J. M. H.; Klein, M. *Interagency Report NBSIR 79-1715*; National Bureau of Standards: 1978.
(29) Straty, G. C.; Palavra, A. M. F. Automated High-Temperature PVT Apparatus with Data for Propane. *J. Res. Natl. Bur. Stand. (U.S.)* **1984**, *89*, 375−383.

(30) Warowny, W.; Wielopolski, P.; Stecki, J. Compressibility Factors and Virial Coefficients for Propane, Propene and Their Mixtures by the Burnett Method. *Physica A* **1978**, *91*, 73−87.
(31) Helgeson, N. L.; Sage, B. H. Latent Heat of Vaporization of Propane. *J. Chem. Eng. Data* **1967**, *12*, 47−49.
(32) Hondo, T.; Kayukawa, Y.; Watanabe, K. *PρTx* Measurements for Gas-Phase Propane + Isobutane System by the Burnett Method. In *Proc. Asian Conf. Refrig. Airconditioning*; Kobe, Japan, December 2002.
(33) Kemp, J. D.; Egan, C. J. Hindered Rotation of the Methyl Groups in Propane. The Heat Capacity, Vapor Pressure, Heats of Fusion and Vaporization of Propane. Entropy and Density of the Gas. *J. Am. Chem. Soc.* **1938**, *60*, 1521−1525.
(34) Kratzke, H. Thermodynamic Quantities for Propane. 1. The Vapour Pressure of Liquid Propane. *J. Chem. Thermodyn.* **1980**, *12*, 305−309.
(35) Magee, J. W. National Institute of Standards and Technology (NIST): Boulder, CO; Private communication, 1999.
(36) Teichmann, J. Ph.D. Thesis, Ruhr University, Bochum, Germany, 1978.
(37) Flebbe, J. L.; Barclay, D. A.; Manley, D. B. Vapor Pressures of Some C4 Hydrocarbons and Their Mixtures. *J. Chem. Eng. Data* **1982**, *27*, 405−412.
(38) Machin, W. D.; Golding, P. D. Vapour Pressure of Butane from 173 to 280 K. *J. Chem. Soc.* **1989**, *85*, 2229−2239.
(39) Beattie, J. A.; Marple, S., Jr.; Edwards, D. G. The Vapor Pressure, Orthobaric Liquid Density, and Critical Constants of Isobutane. *J. Chem. Phys.* **1949**, *17*, 576−577.
(40) Connolly, J. F. Ideality of *n*-Butane:Isobutane Solutions. *J. Phys. Chem.* **1962**, *66*, 1082−1086.
(41) Gilliland, E. R.; Scheeline, H. W. High-Pressure Vapor-Liquid Equilibrium, For the Systems Propylene-Isobutane and Propane-Hydrogen Sulfide. *Ind. Eng. Chem.* **1940**, *32*, 48−54.
(42) Higashi, Y.; Funakura, M.; Yoshida, Y. Vapor-Liquid Equilibrium for Propane/Iso-butane Mixture. In *International Conference, CFCs the Day After*; International Institute of Refrigeration (IIR/IIF): Padova, Italy, 1994; Vol. 2.
(43) Hipkin, H. Experimental Vapor-Liquid Equilibrium Data for Propane-Isobutane. *AIChE J.* **1966**, *12*, 484−487.
(44) Hirata, M.; Suda, S. Saturated Vapor Pressure of Isobutane and *n*-Butane in High-Pressure Regions (in Japanese). *Sekiyu Gakkaishi* **1966**, *9*, 885−889.
(45) Kahre, L. C. Liquid Density of Light Hydrocarbon Mixtures. *J. Chem. Eng. Data*. **1973**, *18*, 267−270.
(46) Lee, B.-G.; Park, J. Y.; Lim, J.-S.; Lee, Y.-W.; Lee, C.-H. Vapor−Liquid Equilibria for Isobutane Plus Pentafluoroethane (HFC-125) at 293.15 to 313.15 K and + 1,1,1,2,3,3,3-Heptafluoropropane (HFC-227ea) at 303.15 to 323.15 K. *J. Chem. Eng. Data*. **2000**, *45*, 760−763.
(47) Leu, A.-D.; Robinson, D. B. Equilibrium Phase Properties of the *n*-Butane−Carbon Dioxide and Isobutane−Carbon Dioxide Binary Systems. *J. Chem. Eng. Data* **1987**, *32*, 444−447.
(48) Leu, A.-D.; Robinson, D. B. Equilibrium Phase Properties of the *n*-Butane−Hydrogen Sulfide and Isobutane−Hydrogen Sulfide Binary Systems. *J. Chem. Eng. Data* **1989**, *34*, 315−319.
(49) Lim, J.-S.; Park, J. Y.; Lee, B.-G.; Lee, Y.-W.; Kim, J.-D. Phase Equilibria of CFC Alternative Refrigerant Mixtures: Binary Systems of Isobutane + 1,1,1,2-Tetrafluoroethane, + 1,1-Difluorethane, and + Difluoromethane. *J. Chem. Eng. Data*. **1999**, *44*, 1226−1230.
(50) Lim, J.-S.; Park, J. Y.; Lee, B.-G.; Kim, J.-D. Phase Equilibria of Chlorofluorocarbon Alternative Refrigerant Mixtures. Binary Systems of Trifluoromethane + Isobutane at 283.15 and 293.15 K and 1,1,1-Trifluoroethane + Isobutane at 323.15 and 333.15 K. *J. Chem. Eng. Data*. **2000**, *45*, 734−737.
(51) Martinez-Ortiz, J. A.; Manley, D. B. Vapor Pressures for the System Isobutane−Isobutylene−*n*-Butane. *J. Chem. Eng. Data* **1978**, *23*, 165−167.
(52) Steele, K.; Polling, B. E.; Manley, D. B. Vapor Pressures for the System 1-Butene, Isobutane, and 1,3-Butadiene. *J. Chem. Eng. Data* **1976**, *21*, 399−403.
(53) Wackher, R. C.; Linn, C. B.; Grosse, A. V. Physical Properties of Butanes and Butenes. *Ind. Eng. Chem.* **1945**, *37*, 464−468.
(54) Weber, L. A. Vapour-Liquid Equilibria Measurements for Carbon Dioxide with Normal and Isobutane from 250 to 280 K. *Cryogenics* **1985**, *25*, 338−342.
(55) Weber, L. A. Simple Apparatus for Vapor−Liquid Equilibrium Measurements with Data for the Binary Systems of Carbon Dioxide with *n*-Butane and Isobutane. *J. Chem. Eng. Data* **1989**, *34*, 171−175.
(56) Weber, L. A. Vapor−Liquid Equilibrium in Binary Systems of Chlorotrifluoromethane with *n*-Butane and Isobutane. *J. Chem. Eng. Data.* **1989**, *34*, 452−455.
(57) Sliwinski, P. Die Clausius-Mosotti-Funktion für die Gesättigten Dämpfe und Flüssigkeiten des Äthans und Propans. *Z. Phys. Chem. Neue. Folge.* **1969**, *68*, 91−98.

Received for review September 13, 2004. Accepted November 28, 2004.

JE049672L